ELSEVIER

Physics of the Earth and Planetary Interiors 84 (1994) 161–178

PHYSICS OF THE EARTH AND PLANETARY INTERIORS

Performance of Wielandt–Streckeisen STS-1 seismometers in the tidal domain—preliminary results

R. Pillet *[,a], N. Florsch [b], J. Hinderer [a], D. Rouland [a]

[a] *Laboratoire de Sismologie, Ecole et Observatoire de Physique du Globe, 5 rue René Descartes, 67084 Strasbourg Cedex, France*
[b] *Laboratoire de Géophysique Appliquée, Université Pierre et Marie Curie, 4 place Jussieu, 75005 Paris Cedex, France*

(Received 1 January 1993; revision accepted 13 December 1993)

Ô, petits gravitons qui passez par Jineuf...
J. Hinderer (1990)

Abstract

The aim of this work is to show that STS-1 seismometers are able to provide a signal with a very long period vertical component which can be used for Earth tide studies provided a number of recording conditions are improved. We use data from the GEOSCOPE network for BNG (Bangui, Central African Republic), MBO (M'bour, Senegal), CRZF (Crozet, TAAF (Terres Australes et Antarctiques Françaises), Indian Ocean), ECH (Echery, France) and PAF (Port-aux-Français, Kerguelen, TAAF, Indian Ocean) stations operated by the Ecole et Observatoire de Physique du Globe de Strasbourg (EOPGS) and Institut Français de Recherche Scientifique pour le Développement en Coopération (ORSTOM). These data are analysed with a least-squares adjustment method to fit the Earth tidal waves, and the results for these stations are compared. Special attention is paid to the comparison of results from ECH with those from the superconducting gravimeter of Strasbourg (J-9). For several stations used in this study (CRZF, MBO and ECH) the results are promising, but they are disappointing for others (PAF and BNG). We did not find any clear reason for such a difference in quality. We propose some improvements that will enable researchers to achieve a better recording of this long-period signal and obtain higher-quality data allowing gravimetric studies from global seismological networks.

1. Introduction

An STS-1 seismometer (Wielandt and Streckeisen, 1982) delivers a voltage signal called POS (Fig. 1) which corresponds to the mass device position. This voltage is proportional to the gravitational acceleration, and the transfer function is flat for periods from infinity to 20 s (360 s for STS-1 seismometers configured in very broad band (VVB) (Wielandt and Steim, 1985)). At the GEOSCOPE (Romanowicz et al., 1984, 1991) stations operated by the Ecole et Observatoire de Physique du Globe de Strasbourg (EOPGS) and the Institute Français de Recherche Scientifique pour le Développement et Cooperation (ORSTOM), we have recorded the three components of POS with a 1 min sampling interval (Pillet et al., 1990). We consider here only the

* Corresponding author.

SSDI 0031-9201(94)05031-R

vertical component (tidal gravity) of POS for the Stations Bangui, Central African Republic (BNG), Crozet, TAAF (Terres Australes et Antarctiques Françaises), Indian Ocean (CRFZ), Echery, France (ECH), M'bour, Senegal (MBO) and Port-aux-Français, Kerguelen, TAAF Indian Ocean (PAF). We intend to show in this study that, under certain conditions, the quality of this signal is comparable with that of a standard spring gravimeter. A potential consequence would be the use of the GEOSCOPE network (and other networks such as IRIS or MEDNET) as a gravimeter network; this would allow gravity changes to be studied on a planetary scale using a large number of stations or stations at unusual locations (Wahr, 1981; Melchior and De Becker, 1983; Dehant and Ducarme, 1987; Cummins et al., 1991).

2. Signal processing

The raw 1 min signal is not fully continuous because of gaps caused by disruptions and resettings. Some glitches are caused by radio transmitting errors (e.g. at ECH) and are removed with the help of the Seismic Analysis Code (SAC) software (Tull et al., 1987). We used the longest uninterrupted continuous signals, because recentring the mass of the seismometer or calibration leads to gaps in POS that have to be eliminated. Each strong earthquake ($M_s > 6$) also produces a

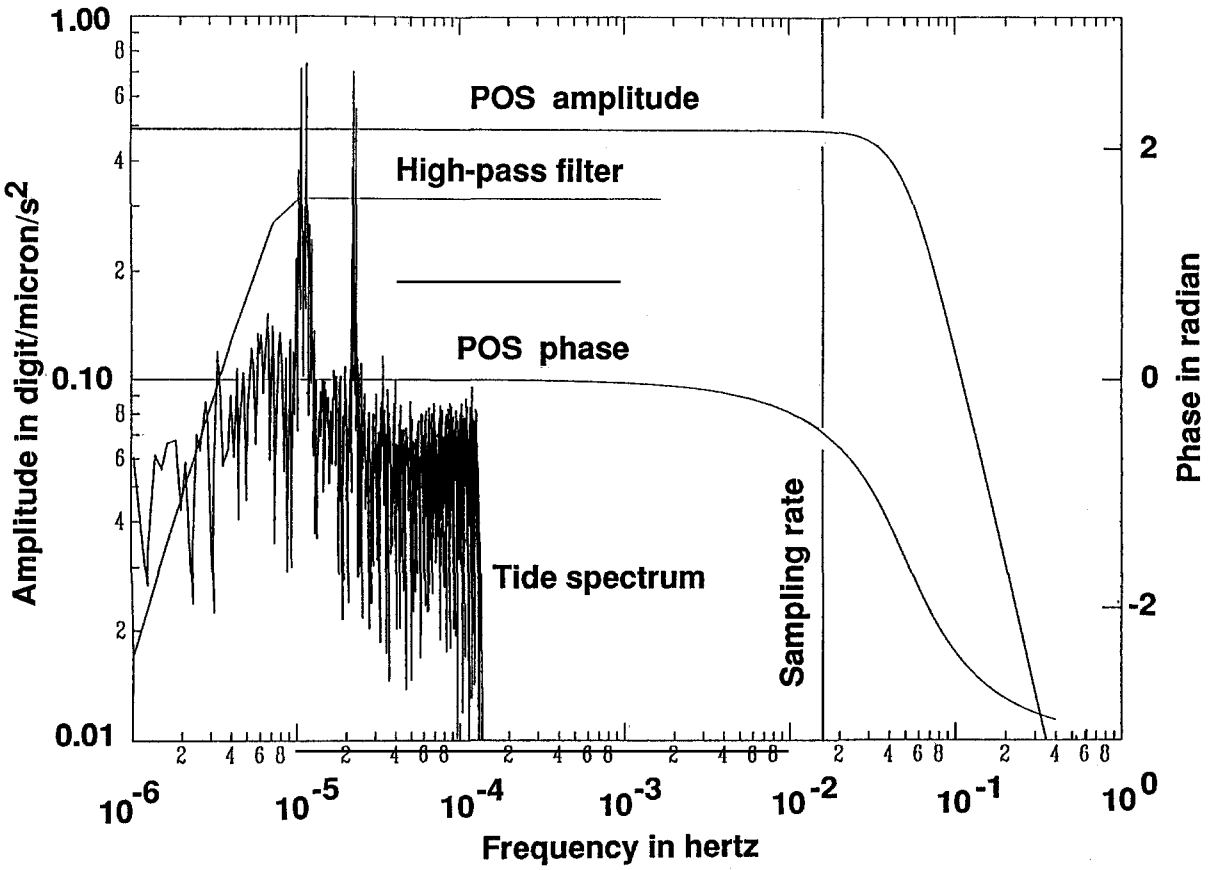

Fig. 1. Bandwidth of POS (amplitude and phase) and convolution high-pass filter with cut-off frequency at 1/46 h. A tidal spectrum is also plotted.

perturbation of POS which is replaced by a gap with null values. An anti-aliasing convolution filter is applied to the raw 1 min data which are then decimated by a factor of five.

To build a longer continuous signal from the available segments is necessary to perform a tidal analysis, and this requires a procedure to fill the gaps. This procedure is based on a least-squares analysis of the signal around the gap (three times the length of the gap before and after it). The model involves the main tidal waves (10 waves) and the inversion is performed by using a singular value decomposition which allows us to analyse time intervals much shorter than that theoretically compatible with the natural spectral resolution of the model. For instance, let us suppose a gap length of 1 day. Six days are used in the inversion, although only two or three waves can be modelled with this duration. Filling gaps longer than 1 day using the method described above seems doubtful, and we tried to avoid such circumstances.

The output POS is directly proportional to the gravitational acceleration (the phase lag vanishes; see Fig. 1) and the data are multiplied by the scale factors given by the manufacturer. High drifts may occur in the signal as a result of temperature influence on the spring. In this case, tidal waves hardly emerge from the noise. To eliminate this drift, the data are filtered through a high-pass convolution (FIR) filter with a cut-off period of 46 h (Fig. 1). This filter fully preserves the amplitude of the diurnal tidal waves (as well as semi-diurnal and ter-diurnal waves). The re-

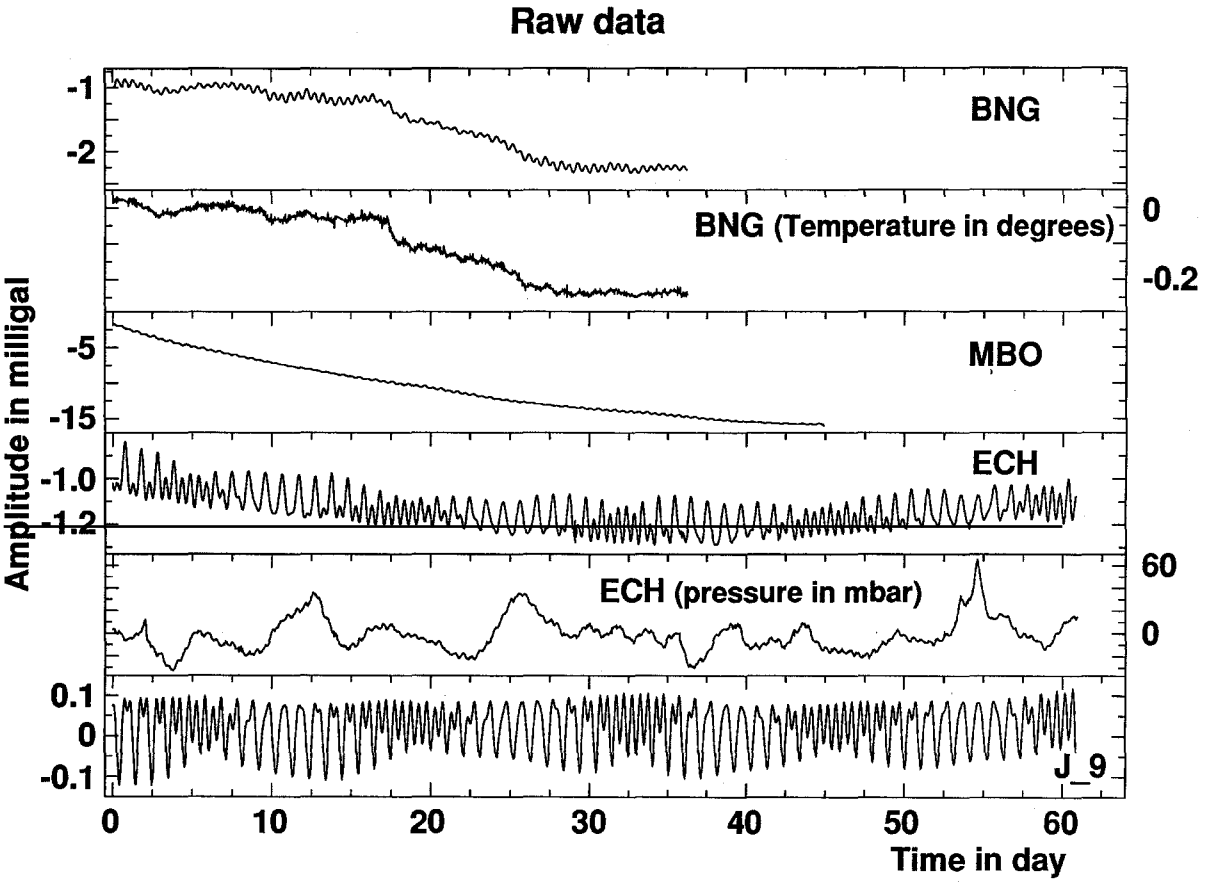

Fig. 2. Raw data at BNG, MBO, ECH and J-9 with, in addition, the temperature at BNG and the pressure at ECH. The durations are between 1 and 2 months.

sulting signal is shown below, in Fig. 5, where the classical pattern of tidal beating can be seen.

3. Tidal analysis

We perform the tidal analysis by using the program HYCON (Schüller, 1985), which computes the amplitudes and phases of the observed tidal waves by a least-squares method and provides for each station and tidal group the gravimetric amplitude factors δ and phase differences κ (Melchior, 1978). The waves are grouped, to take into account the resolution depending on the duration of the signal. In our case, three tidal bands (diurnal, semi-diurnal and ter-diurnal) with 17 wave groups are considered. Although HYCON allows us to introduce a low-degree polynomial drift, we do not use this possibility. Indeed, low-frequency components have already been eliminated by the high-pass filtering. Moreover, some attempts to remove the drift by using a polynomial fit were not satisfactory.

We present our results in two sets. The first set includes four stations (BNG, MBO, ECH and the Strasbourg station J-9) and corresponds to a signal duration of about 1 month. The raw data are displayed in Fig. 2. The temperature at BNG and the pressure at ECH are also plotted. At J-9, the pressure is recorded but not plotted, as it is very similar to that at ECH (the distance between the two stations is only 60 km). It should be noted

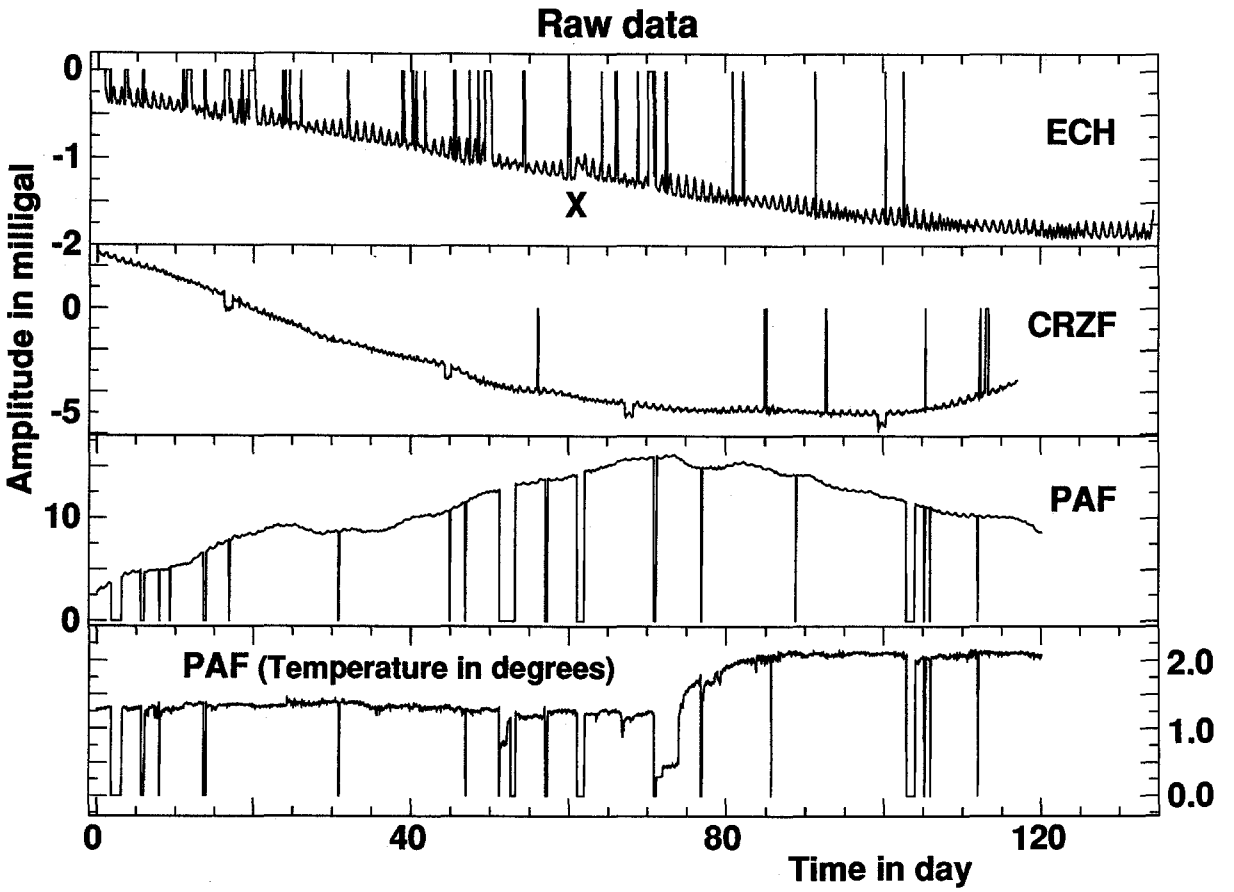

Fig. 3. Raw data at ECH, CRZF and PAF with temperature at PAF. These signals are plotted before interpolating the gaps. The duration is about 3 months. On ECH, the disturbance marked X should be noted.

that the POS signal at BNG closely follows the temperature signal. The drift at MBO is very high but regular, in agreement with the slow evolution of the temperature in a well-isolated room. However, because of maintenance requirements, transient signals can occur that reach 10 mV or more in the POS signal.

The second set includes data from ECH, CRZF and PAF, for which the data last about 3 months (Fig. 3). We show these data before filling gaps and pre-processing. Thermal drifts are small (ECH), medium (CRZF) or high (PAF). At PAF, we have also the inner instrument temperature, which is not in good agreement with the signal provided by this seismograph, in contrast to the BNG case. We believe that the recording process of this temperature signal has been modified. On ECH data, the zone marked X contains a disturbance of unknown cause; the effect of this perturbation will be seen below.

In this study, we will focus on the vertical component of the STS-1 seismometers. A similar study could be extended to the horizontal components, at least for some stations such as MBO where horizontal tides are as well recorded as vertical tides (see Fig. 4).

Figs. 5 and 6 show the signal after pre-processing. The diurnal/semi-diurnal beats clearly appear, except for the PAF signal, which is very noisy. The changes in temperature and pressure are usually more smooth, except when a disruption occurs. As previously noted these data sets have been analysed by HYCON, and Table 1 gives the results. We present only the waves that have root mean square (r.m.s.) errors less than 0.1 unit for the amplitude and less than 5° for the phase. The parameters specified in the tidal fitting code HYCON are identical for all the analyses shown, but because of the above-mentioned selection criteria, the number of waves for which

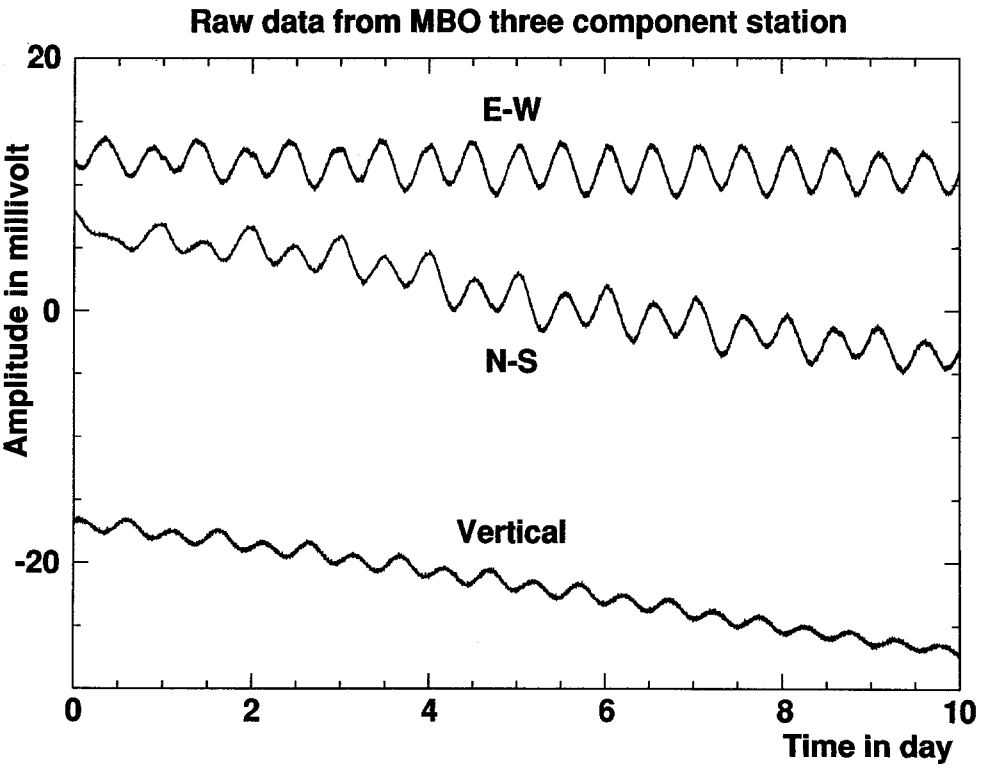

Fig. 4. Raw data from MBO three-component station. The tides are clearly visible on both vertical and horizontal components.

Table 1
Tidal analysis results provided by the HYCON least-squares fitting code; we kept the waves for which r.m.s. (δ) < 0.1 and r.m.s. (κ) < 5° (HYCON gives the r.m.s. residual level in microgal in the three diurnal, semi-diurnal and ter-diurnal frequency bands, as well as in the full frequency band). c(95)% is the 95% confidence interval

(a) Bangui station (BNG); 2 December 1989; 30 days; Lat. +04.435°; Long. +18.546°

No.	Tide	δ	r.m.s.	c (95%)	κ	r.m.s.	c (95%)
6	K1	1.6709	0.1106	0.2293	−35.79	2.90	6.00
13	M2	0.5631	0.0183	0.0380	14.51	1.86	3.87

Diurnal	1.Spectr.domain: 11.9–16.9 degrees h^{-1} MO = 11.35 μgal
Semi-diurnal	2.Spectr.domain: 26.8–31.8 degrees h^{-1} MO = 22.50 μgal
Ter-diurnal	3.Spectr.domain: 42.2–47.2 degrees h^{-1} MO = 3.46 μgal
Sum	4.Spectr.domain: 0.0–180.0 degrees h^{-1} MO = 6.24 μgal

MO = equivalent time standard deviation
Temperature also recorded.
Many interruptions (possible long).

(b) M'Bour station (MBO); 22 December 1988; 39 days; Lat. +14.390°; Long −16.955°

No.	Tide	δ	r.m.s.	c (95%)	κ	r.m.s.	c (95%)
4	O1	1.1415	0.0252	0.0516	−3.31	1.26	2.59
6	K1	1.0900	0.0154	0.0315	−16.08	0.81	1.65
12	N2	1.2390	0.0266	0.0545	−0.96	1.23	2.52
13	M2	1.1963	0.0044	0.0090	−1.70	0.21	0.43
15	S2	1.3154	0.0111	0.0226	3.58	0.48	0.99
17	M3	0.9582	0.0849	0.1739	4.24	5.08	10.40

Diurnal	1.Spectr.domain: 12.0–17.0 degrees h^{-1} MO = 8.42 μgal
Semi-diurnal	2.Spectr.domain: 27.1–32.1 degrees h^{-1} MO = 5.72 μgal
Ter-diurnal	3.Spectr.domain: 42.1–47.2 degrees h^{-1} MO = 1.99 μgal
Sum	4.Spectr.domain: 0.0–180.0 degrees h^{-1} MO = 3.08 μgal

(c)Echery station (ECH); 17 August 1989; 55 days; Lat. +48.216°; Long −07.158°

No.	Tide	δ	r.m.s.	c (95%)	κ	r.m.s.	c (95%)
3	Q1	1.2035	0.0504	0.1019	−1.63	2.40	4.85
4	O1	1.1507	0.0109	0.0220	−0.88	0.54	1.10
5	M1	1.2272	0.0975	0.1974	14.70	4.55	9.22
6	K1	1.1512	0.0109	0.0220	2.21	0.54	1.10
7	J1	1.4698	0.1208	0.2446	1.75	4.71	9.53
12	N2	1.1373	0.0273	0.0552	0.77	1.38	2.78
13	M2	1.1497	0.0059	0.0120	1.82	0.30	0.60
15	S2	1.1814	0.0119	0.0241	1.88	0.64	1.29

Diurnal	1.Spectr.domain: 12.1–17.0 degrees h^{-1} MO = 7.99 μgal
Semi-diurnal	2.Spectr.domain: 26.9–32.1 degrees h^{-1} MO = 4.05 μgal
Ter-diurnal	3.Spectr.domain: 41.9–46.9 degrees h^{-1} MO = 2.13 μgal
Sum	4.Spectr.domain: 0.0–180.0 degrees h^{-1} MO = 2.42 μgal

Pressure also recorded.

(d) Strasbourg station (J-9); 17 August 1989; 55 days; Lat. +48.622°; Long −07.684°

No.	Tide	δ	r.m.s.	c (95%)	κ	r.m.s.	c (95%)
1	SIQ1	1.0715	0.0468	0.0948	−3.13	2.50	5.07
2	SIG1	1.1207	0.0092	0.0186	−0.75	0.47	0.95
3	Q1	1.1353	0.0020	0.0041	−0.56	0.10	0.21
4	O1	1.1425	0.0004	0.0009	−0.12	0.02	0.04
5	M1	1.1494	0.0039	0.0079	−0.32	0.19	0.39

Table 1 (continued)

No.	Tide	δ	r.m.s.	c (95%)	κ	r.m.s.	c (95%)
6	K1	1.1369	0.0004	0.0009	0.20	0.02	0.04
7	J1	1.1640	0.0048	0.0098	0.07	0.24	0.48
8	OO1	1.1518	0.0056	0.0113	0.05	0.28	0.56
9	V1	1.1492	0.0283	0.0573	−0.93	1.41	2.86
10	EPS2	1.1511	0.0336	0.0680	1.61	1.67	3.38
11	2N2	1.1529	0.0065	0.0132	2.68	0.33	0.66
12	N2	1.1766	0.0014	0.0029	2.20	0.07	0.14
13	M2	1.1850	0.0003	0.0006	1.79	0.02	0.03
14	L2	1.2603	0.0151	0.0307	0.16	0.69	1.39
15	S2	1.1893	0.0005	0.0010	0.43	0.02	0.05
16	ETA2	1.2124	0.0243	0.0492	−1.42	1.15	2.32
17	M3	1.0624	0.0266	0.0539	−0.02	1.43	2.90

Diurnal	1.Spectr.domain: 12.0–16.9 degrees h^{-1} MO = 0.32 μgal
Semi-diurnal	2.Spectr.domain: 27.1–32.0 degrees h^{-1} MO = 0.21 μgal
Ter-diurnal	3.Spectr.domain: 42.1–47.0 degrees h^{-1} MO = 0.23 μgal
Sum	4.Spectr.domain: 0.0–180.0 degrees h^{-1} MO = 0.14 μgal

Pressure also recorded.

(e) Echery station (ECH); 10 May 1990; 127 days; Lat. +48.216°; Long −07.158°

No.	Tide	δ	r.m.s.	c (95%)	κ	r.m.s.	c (95%)
3	Q1	1.1966	0.0497	0.0988	−1.08	2.38	4.73
4	O1	1.1234	0.0097	0.0192	−2.42	0.49	0.98
6	K1	1.0922	0.0063	0.0126	0.35	0.33	0.66
7	J1	1.3825	0.1127	0.2239	−1.57	4.67	9.28
12	N2	1.1299	0.0267	0.0531	0.40	1.35	2.69
13	M2	1.1577	0.0055	0.0109	0.36	0.27	0.54
15	S2	1.2189	0.0130	0.0259	0.54	0.61	1.22

Diurnal	1.Spectr.domain: 11.9–17.0 degrees h^{-1} MO = 10.78 μgal
Semi-diurnal	2.Spectr.domain: 27.0–31.9 degrees h^{-1} MO = 5.72 μgal
Ter-diurnal	3.Spectr.domain: 42.0–47.0 degrees h^{-1} MO = 2.23 μgal
Sum	4.Spectr.domain: 0.0–180.0 degrees h^{-1} MO = 3.05 μgal

Signal perturbed by radio link glitches.

(f) Crozet station (CRZF); 16 February 1989; 111 days; Lat. −46.430°; Long −51.861°

No.	Tide	δ	r.m.s.	c (95%)	κ	r.m.s.	c (95%)
3	Q1	1.1455	0.0300	0.0597	2.76	1.50	2.98
4	O1	1.1839	0.0065	0.0129	−0.42	0.31	0.62
5	M1	1.1663	0.0534	0.1064	−1.13	2.62	5.23
6	K1	1.1309	0.0053	0.0106	0.29	0.27	0.54
7	J1	1.2409	0.0756	0.1506	7.61	3.49	6.95
8	OO1	1.0685	0.0845	0.1683	3.63	4.53	9.02
11	2N2	1.2675	0.0705	0.1405	4.80	3.19	6.35
12	N2	1.2466	0.0164	0.0326	−2.29	0.75	1.50
13	M2	1.2062	0.0035	0.0069	−3.37	0.16	0.33
14	L2	1.0925	0.0944	0.1880	−3.91	4.95	9.86
15	S2	1.1708	0.0060	0.0120	−1.70	0.30	0.59

Diurnal	1.Spectr.domain: 12.0–17.0 degrees h^{-1} MO = 6.88 μgal
Semi-diurnal	2.Spectr.domain: 27.0–32.0 degrees h^{-1} MO = 3.56 μgal
Ter-diurnal	3.Spectr.domain: 42.0–47.0 degrees h^{-1} MO = 2.61 μgal
Sum	4.Spectr.domain: 0.0–180.0 degrees h^{-1} MO = 3.18 μgal

Four disturbances caused by calibration tests.
Temperature recording out of scale.

Table 1 (continued)
(g) Kerguelen station (PAF); 24 July 1990; 110 days; Lat. −49.305°; Long −70.213°

No.	Tide	δ	r.m.s.	c (95%)	κ	r.m.s.	c (95%)
4	O1	0.9590	0.0902	0.1796	−4.88	5.38	10.73
6	K1	1.2243	0.0815	0.1623	−3.01	3.81	7.60
13	M2	0.9899	0.0240	0.0477	−6.79	1.39	2.76
15	S2	0.9566	0.0407	0.0811	0.14	2.44	4.86

Diurnal 1.Spectr.domain: 12.0–17.1 degrees h^{-1} MO = 92.40 μgal
Semi-diurnal 2.Spectr.domain: 26.9–32.0 degrees h^{-1} MO = 22.25 μgal
Ter-diurnal 3.Spectr.domain: 42.0–47.0 degrees h^{-1} MO = 9.96 μgal
Sum 4.Spectr.domain: 0.0–180.0 degrees h^{-1} MO = 25.09 μgal
Two disturbances caused by recentering of the mass.
Three disturbances caused by calibration tests.
Temperature also recorded.

results are given is variable. We also give the r.m.s. noise level in different frequency bands: diurnal, semi-diurnal and ter-diurnal, as well as in the full frequency band (from zero to the Nyquist frequency). In the three last lines of Table 1, it can be seen that ECH and CRZF

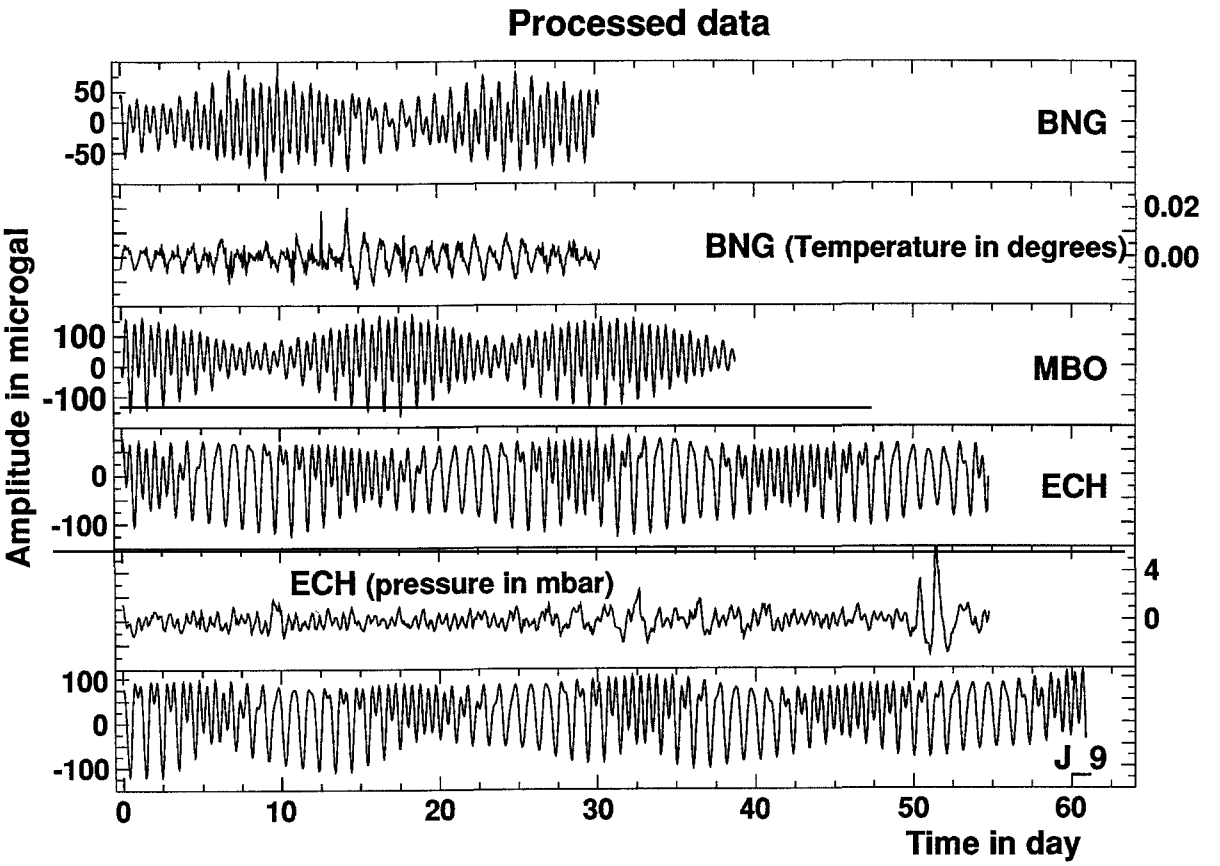

Fig. 5. Processed data at BNG, MBO, ECH and J-9 with the temperature at BNG and the pressure at ECH. The durations are between about 1 and 2 months.

provide good-quality data, but those from PAF are rather disappointing. As pointed out by Agnew and Berger (1978), the noise levels on the gravimeters of the IDA network are higher for stations on islands. This would explain why the PAF signal is noisy. The same should apply to CRZF; however, this is not the case and we are therefore left with additional noise sources owing to poor atmospheric conditions at this station and/or to an inadequate thermal shielding of the cave in which the instrument is located.

The actual values of δ and κ are sometimes doubtful, in spite of the chosen r.m.s. threshold proposed for wave selection (e.g. see the BNG data). We found δ factors varying from 0.56 to 1.67 and κ between $-36°$ and $+14°$. These values, which are determined with acceptable formal uncertainties, are very different from the classical expected values related to a standard Earth model ($\delta = 1.16$ and $\kappa = 0°$) (Melchior, 1978; Wahr, 1981). The gravity effect caused by oceanic loading can partially explain these differences, especially for coastal sites such as MBO. However, at BNG the POS signal is often interrupted, sometimes for a long time (12 h or more). The program for filling the gaps is a powerful tool for short time gaps, but fails when an extreme situation is encountered, as at BNG. In addition, at this station, time errors might also have occurred. The results from MBO are in good agreement with those provided by a LaCoste–Romberg gravimeter operated at the same site by the Observatoire Royal de Belgique; for instance, the values relative to the semi-diurnal wave M2 found

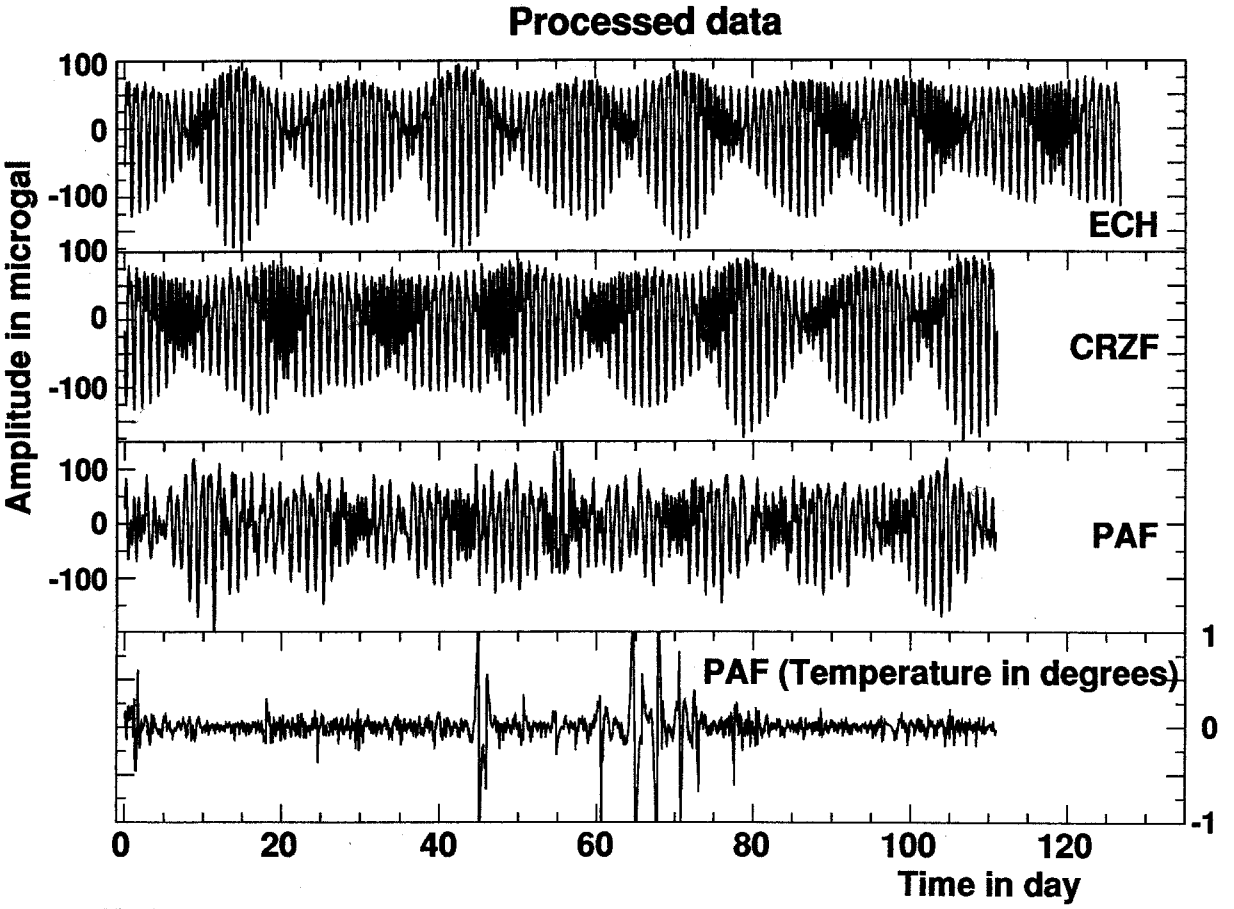

Fig. 6. Processed data at ECH, CRZF and PAF with the temperature at PAF. The duration is about 3 months.

from a 227 day spring gravimeter data set are $\delta = 1.1993 \pm 0.0027$ and $\kappa = -1.58 \pm 0.13°$ (P. Melchior, personal communication, 1992), and are within the error bars of the seismometer results (see Table 1).

4. Comparison of results from different stations

Two signals have been processed at the same station, ECH; one is 55 days long and the other lasts 127 days without any overlap. The results (δ and κ values) for the main waves obtained from the tidal fitting code HYCON are shown in Fig. 7. For the waves of small amplitude with a large uncertainty, the results overlap, but for large-amplitude waves (such as K1) the differences between the two sets of results can be greater than the r.m.s. values provided by HYCON. It should be noted that these r.m.s. values are only formal errors from the least-squares method and do not include the effects of disturbances in the signal itself; in other words, the r.m.s. values may well be underestimated. Two major reasons explain why the results relative to the same station differ —the different time duration and the fact that the shorter data set (55 days) was corrected for local atmospheric pressure whereas the longer data set was not (the pressure was not available).

In Fig. 8, which shows the results of the comparison between ECH and J-9 (a superconducting gravimeter), we observe two main features: (1) the error ellipses for ECH are always much larger than those for J-9—this shows effect on tidal fitting of the larger residual noise (see Table 1); (2) the values of δ and κ from ECH are, in general, more scattered away from the origin ($\delta = 1.16$ and $\kappa = 0°$) than those from J-9, except for N2 and M2. The main reason for the difference in the tidal results between these two stations, which are geographically close (less than 100 km), is, in our opinion, the quality of the instruments (the time duration is the same and both records have been corrected for pressure). As previously noted, any deviation of the δ and κ factors has first to be corrected for ocean loading

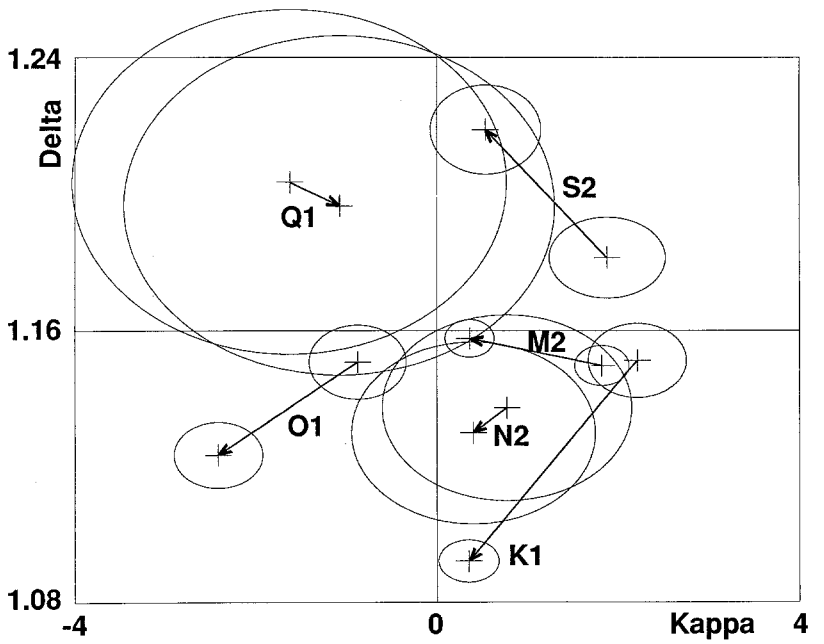

Fig. 7. Comparison between analysis of two sets of data at ECH, the durations being 55 and 127 days, respectively. The ellipses show the r.m.s. errors on the gravimetric amplitude and phase factors. The arrows start at the location of the results for the shorter duration (55 days) and end at the location of the results for the longer duration (127 days).

before being interpretable in terms of the Earth's (an-)elasticity or other physical properties (e.g. Rydelek et al., 1991).

The tidal residual signals from the least-squares fit are shown in Figs. 9 and 10. The amplitude of the residuals at PAF is 10 times larger than those obtained at MBO and ECH. At BNG, the amplitude of residuals is also 10 times larger than those from MBO and ECH, which in turn are 10 times larger than those at J-9. It should be noted that the mean residual level is about 2.5 μgal at ECH, whereas it is actually some tens of nanogals at stations using LaCoste-Romberg gravimeters (Zürn et al., 1991) or superconducting gravimeters (Richer, 1986; Ducarme et al., 1986; Florsch et al., 1991). The spectra of residuals (Figs. 11 and 12) correspond to various resolutions depending on the signal duration for a given station. For instance, semi-diurnal waves are better modelled at CRZF than at ECH or MBO. These components are badly modelled at BNG and PAF. The residual spectrum amplitude is 20 times smaller at J-9 than at ECH for the same period.

Fig. 13 shows the effect of the atmospheric pressure on the signal at ECH. Signal A is the tidal analysis residual obtained without any correction for the pressure signal C (note the large oscillation at the end). Introducing the pressure signal as an additional channel in the HYCON least-squares code leads to the fitted value of the barometric admittance (close to 0.3 μgal/mbar^{-1}), allowing correction for gravity changes induced by local pressure fluctuations. The corresponding residuals are plotted as B: the above-mentioned oscillation disappears and, because of the reduction in the average noise, an additional tidal wave was able to reach the threshold we defined for selection of significant waves.

The top signal on Fig. 14 is the tidal analysis

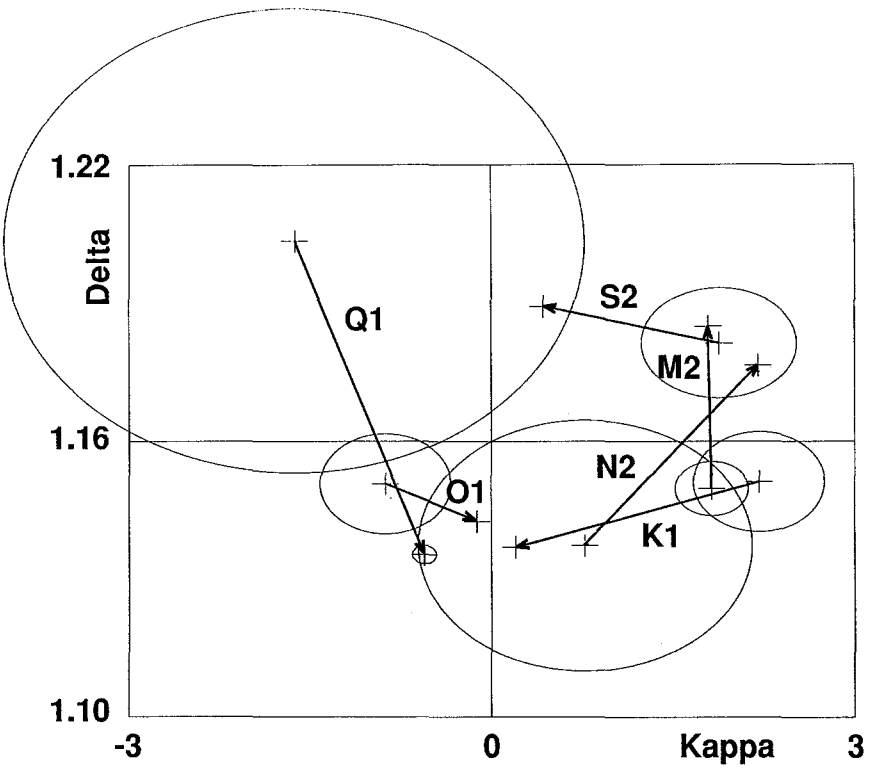

Fig. 8. Comparison of the results obtained at ECH (55 days) and at J-9 (55 days). The ellipses represent the r.m.s. errors on gravimetric amplitude and phase factors. The arrows start at the location of the results for ECH and end at the location of the results for J-9.

residual at ECH without any correction of the disturbance marked X in Fig. 3. It can be seen that the residual signal is highly perturbed around this offset and that there are bursts of noise spread over the signal, especially at the locations marked 1, 2 and 3. When correcting the X disturbance before the tidal least-squares adjustment, the residual signal is much cleaner at the noisy locations, as shown in the lower curve of Fig. 14. The correction technique was, however, extremely rough: we have simply introduced a gap of a few hours at the location of the disturbance and filled it with a synthetic tide plus a linear drift. A better correction could be made by first determining the value of the offset (if any) at the location X before introducing the gap; however, finding the right amplitude offset is difficult and we did not investigate this point further. This example clearly shows the limit in using STS-1 seismometers in the tidal domain, where similar offsets often occur and remain difficult to fully remove.

If the interpretation of the tidal results in terms of global geodynamics is certainly premature, we have been able to show that the STS-1 seismometers provide a gravity signal of interest. However, much work remains to be done before the quality of the measurements (and recordings) can fully compete with results from good tidemeters. We describe below several uncertainty

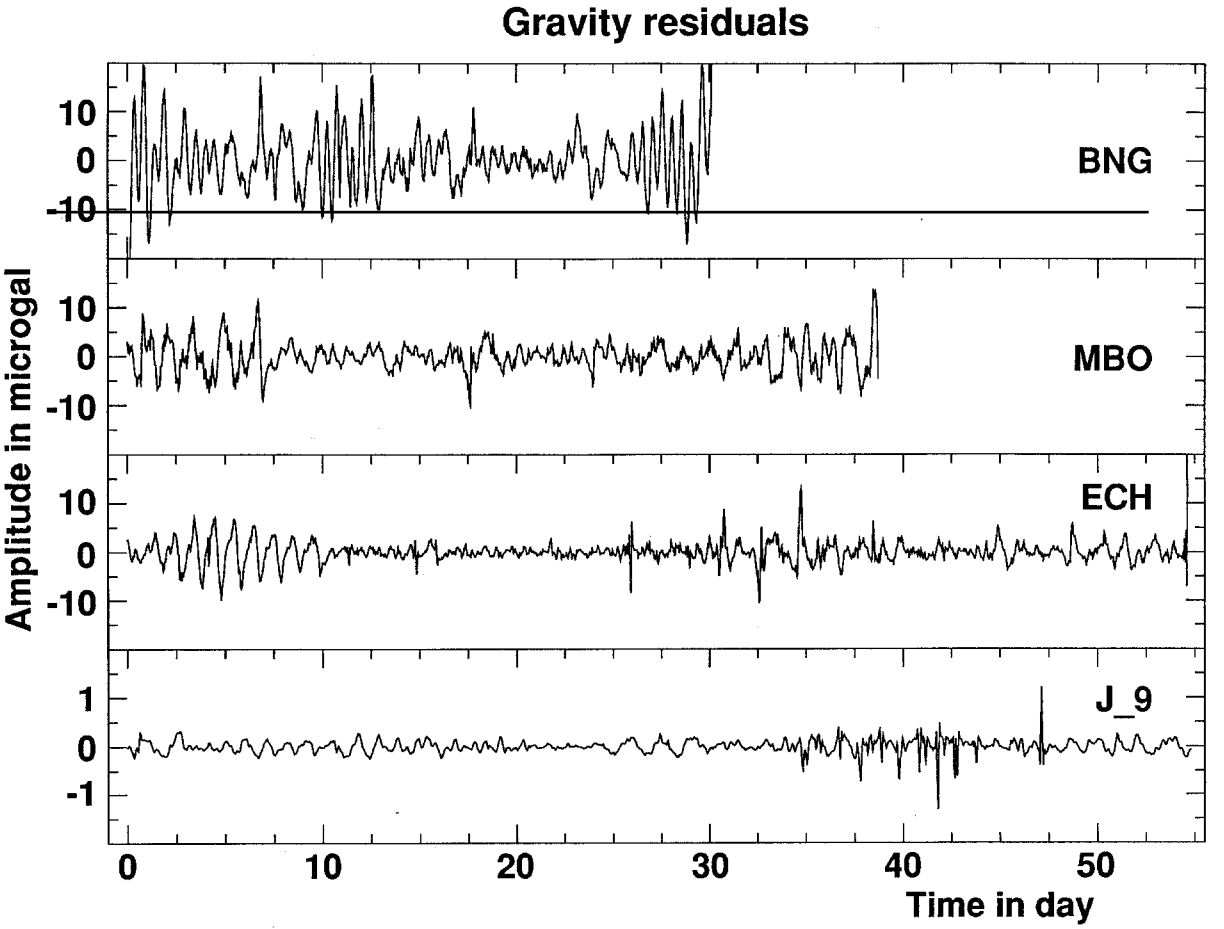

Fig. 9. Tidal residuals at BNG, MBO, ECH and J-9. The scale factor for J-9 is 10 times smaller than the others.

sources degrading the measurements of the STS-1 seismometers which could be at least partly corrected for in the future.

5. Uncertainty sources

5.1. Calibration

One major problem in tidal research is the calibration of the instruments. One needs an extremely precise calibration factor (ideally better than one part per mil) before extracting useful information on the Earth's dynamics from the measurements of tidal amplitudes (see, e.g. Hinderer and Legros, 1989). Only recently, calibration methods using a parallel registration with absolute gravimeters or other well-calibrated relative meters have been tested for gravimeters which guarantee calibration factors slightly better than 1% (see, e.g. Hinderer et al., 1991; Wenzel et al., 1991). In this study we have used the calibration factor given by the manufacturer, which has a nominal uncertainty of the order of 1% (before installation). It is clear that the previous method could be applied to calibrate better the STS-1 seismometers (for an alternative procedure, see also Bernard et al. (1991)). Obviously,

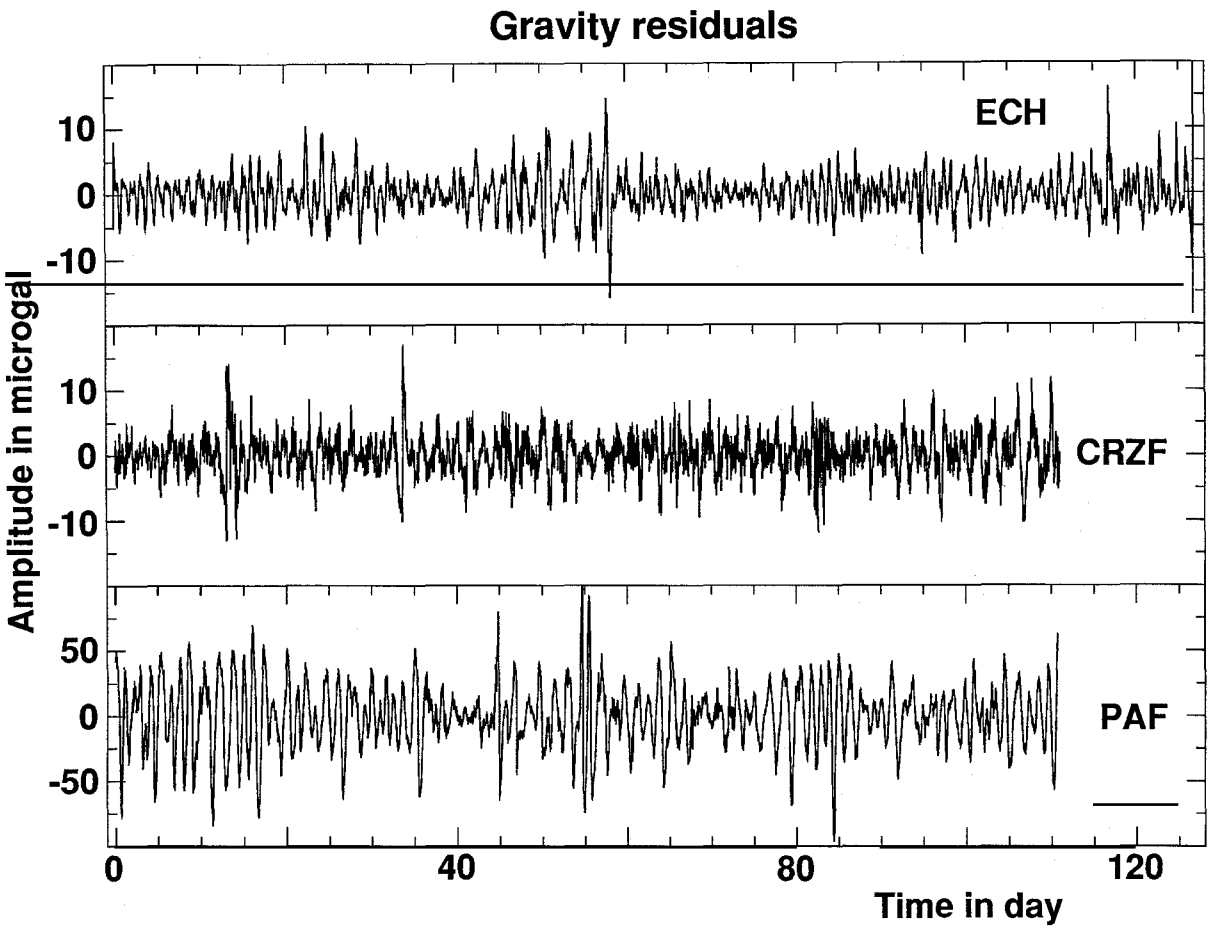

Fig. 10. Tidal residuals at ECH, CRZF and PAF. The duration is about 120 days. The scale for PAF is five times larger than the others.

the consequence of calibration errors would be to extend the error ellipses of Fig. 7 and 8 into ovals lengthened in the direction of δ.

5.2. Twelve-bit digitization and adaptive gain-ranging

For the GEOSCOPE stations maintained by Strasbourg, the voltage proportional to POS is digitized by a 12-bit analog-to-digital converter with an adaptive 2^N gain with $N = 10$ (Pillet et al., 1990). This means that a signal varying between -10 mV and 10 mV is quantized in digits of about 5 μV and that a signal close to 500 mV is represented by digits of 300 μV, i.e. 2^6 (64) times greater (over 500 mV, the instrument is re-centred and the POS signal is then centred around the zero voltage). The signal is less well described when it is far from 0 V; this is a first source of uncertainty. The variable gain is an analog operation, and the gain, which equals theoretically a power of two, has not exactly this value, so that we have a second source of uncertainty. A 24-bit (VBB) acquisition system should cancel this uncertainty, which is difficult to estimate. The analog signal range cannot be set close to the maximum tide amplitude, because one must take in account the thermal drift, which can reach several times the tidal amplitude. However, the magnification of the signal POS could be increased by a factor of 10–20 at some stations.

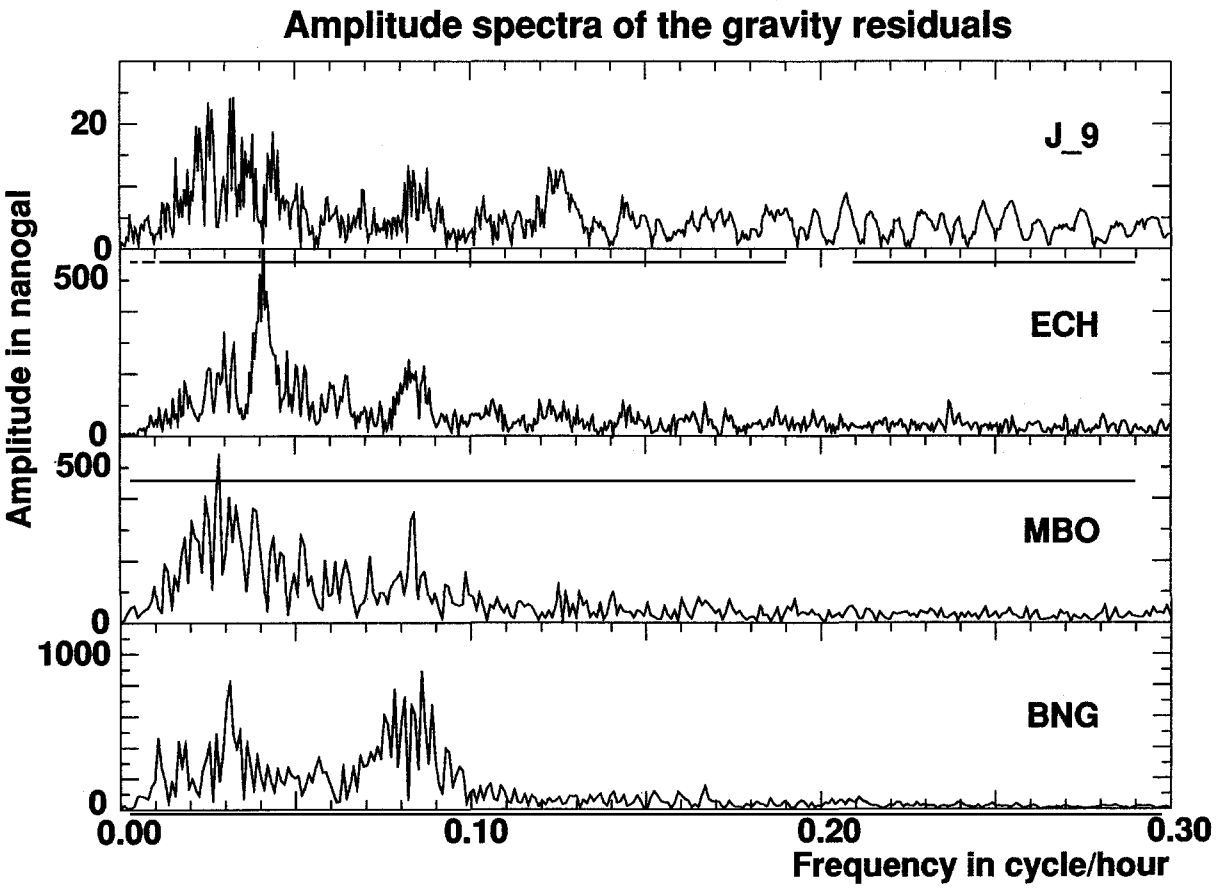

Fig. 11. Comparison of the amplitude spectra of tidal residuals at J-9, ECH, MBO and BNG. The corresponding time duration is about 1 month. (Note the difference in the scale factors between J-9 and the other stations.)

5.3. Clock drift

The numerical recording devices were originally designed for seismic signals. For seismic studies, a small drift is not embarassing. However, when dealing with tides, the observed signal has to last at least 1 month. Over this duration, clock resets often occur. A high clock drift may cause time lags of several seconds, which have an effect on the sampling interval.

5.4. Thermal stability

The thermal shielding limits the temperature variation in time (dT/dt). When this insulation is efficient, the thermal perturbation frequency content is cut down by the high-pass filtering (cut-off frequency of 1/46 h), which is used in this study. This shows that if one wants to deal with longer signals, a better thermal stability should be obtained or better temperature corrections made. Each entrance of the cave where the instrument lies leads to an induced thermal drift so important that it cannot be removed by a simple filtering procedure.

5.5. Quality of the seismic site

The sites where seismic stations are established are generally better than those of gravimetric stations, especially when considering the short-period noise. For instance, ECH is buried

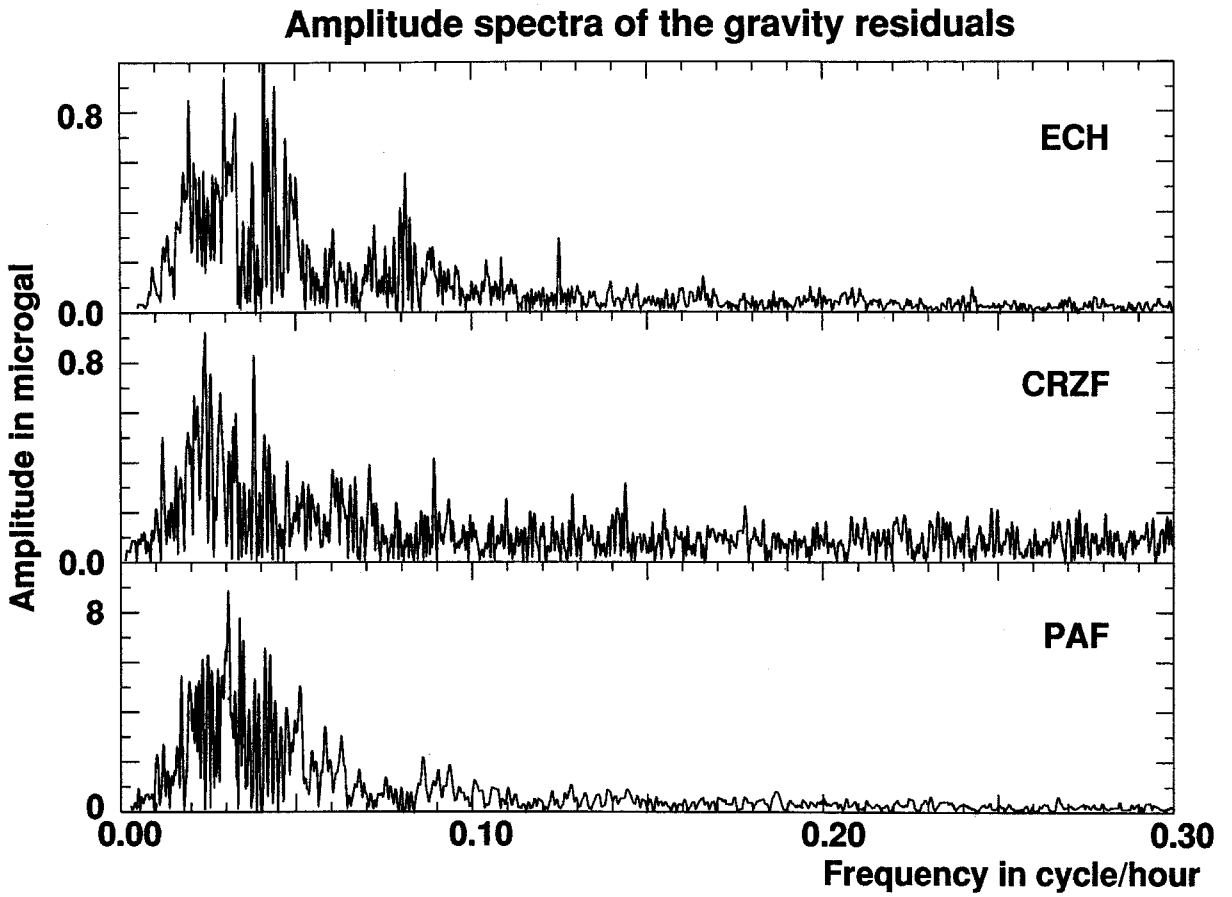

Fig. 12. Comparison between the spectra of tidal residuals at ECH, CRZF and PAF. The corresponding time duration is close to 120 days. The short-period high-level noise at PAF was possibly induced by adverse meteorological conditions.

in a gneissic rock mass whereas J-9 is located close to Strasbourg, in the Rhine sedimentary basin. In addition, proximity to the oceans obviously decreases the quality of some of the stations used in this study.

5.6. Continuity of the record

Although the numerical recording system at EOPGS has been designed to provide a signal without interruption, some problems sometimes occur as a result of the use of low-quality portable microcomputers, which are not initially designed for such continuous work. The resulting gaps are not harmful when processing the seismic signal, but the signal POS must be interpolated in these gaps to allow the analysis of long-period signals such as tides.

5.7. Absence of anti-aliasing filter

We do not think that the absence of anti-aliasing filter is problematic: the ratio of seismic noise (close to the Nyquist period of 2 min) to tidal amplitude is in general extremely low, of the order of −100 dB for BNG and PAF, as shown by Pillet et al. (1990). This is, of course, not true when an earthquake occurs and, in this case, large-amplitude accelerations can be easily aliased and would corrupt the rest of the low-frequency

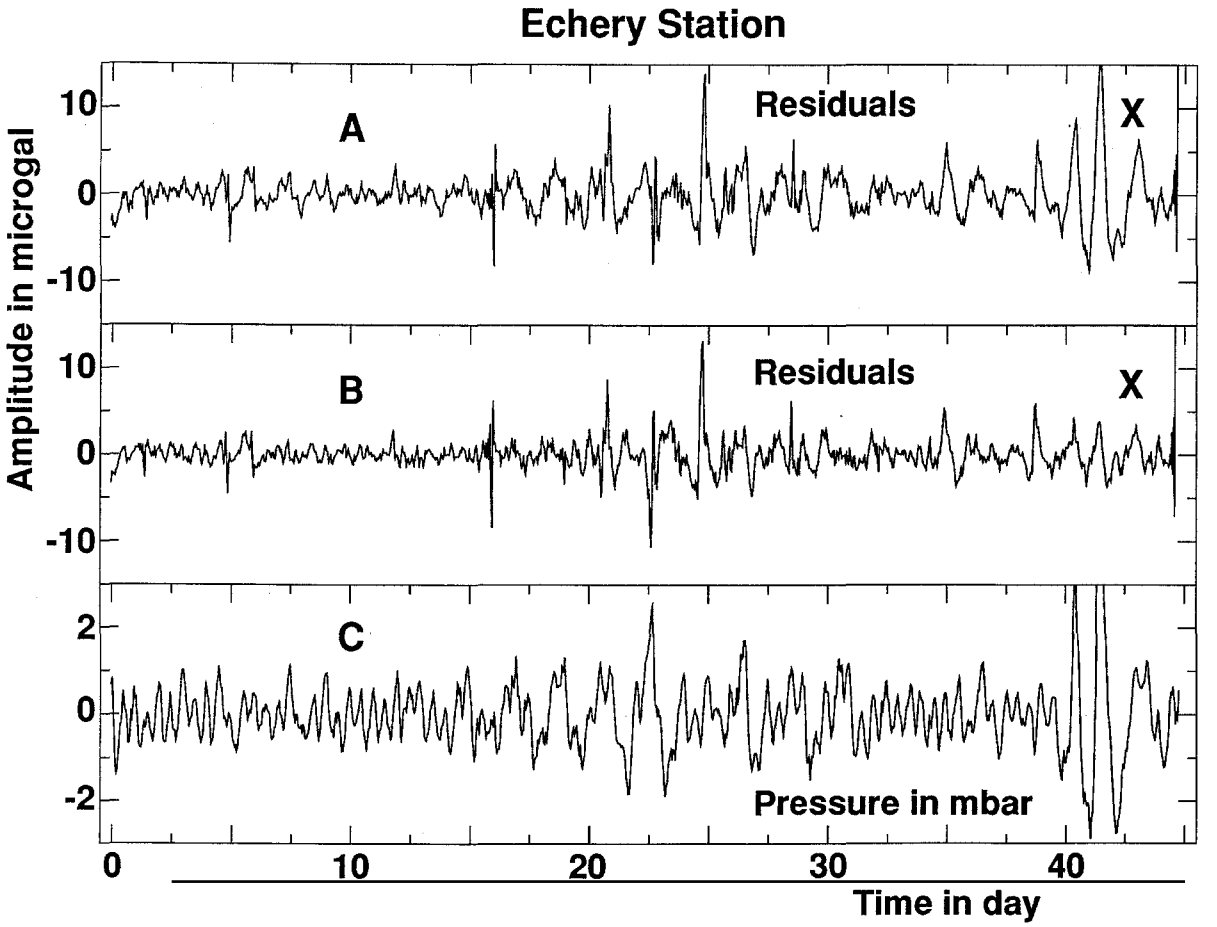

Fig. 13. Pressure influence at ECH: the signal A shows the gravity residuals without any correction of the pressure, C, and the signal B is after pressure correction. The noise reduction is very clear at the end of the signal (marked X).

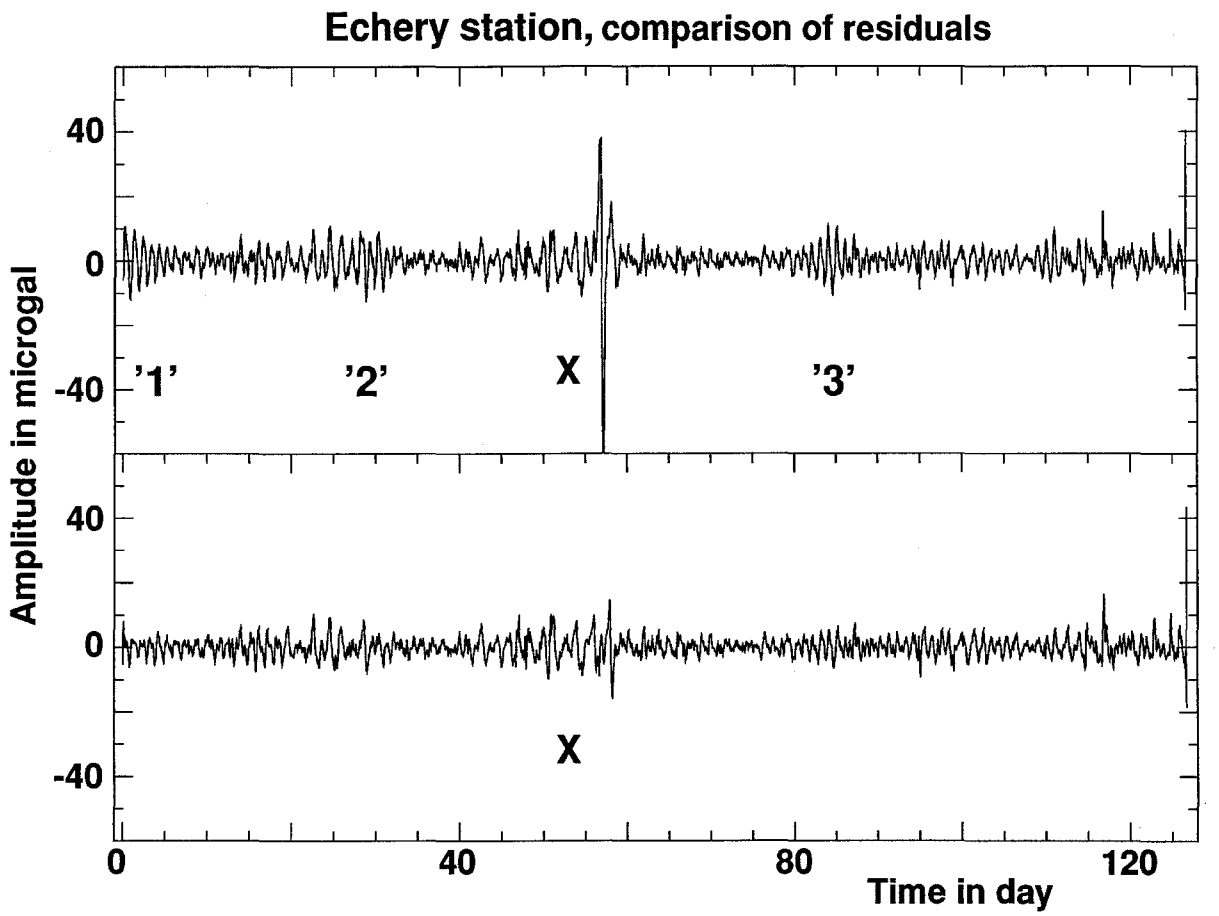

Fig. 14. The upper signal is the residual signal at ECH without correcting for the disturbance X in Fig. 3 before the tidal fit. The lower curve shows the residuals after correction. (Note the reduction of the noise peak close to the area X and the attenuation of the noisy segments marked '1', '2' and '3'.)

signal, including tides. However, during this transient event, a gap is forced, and is refilled by interpolation. The STS-1 configuration in VBB offers a flat band-pass from infinity to 6 min and a roll-off rate of 3 dB per octave. In this latter configuration, the signal POS is weak, but a minimum anti-aliasing filtering would clearly improve the numerical recording.

5.8. Recording POS instead of LP + and LP −

The voltage POS is defined with respect to the mass and is composed from only one (LP −) of the two differential voltages available on the seismometer. This technique reduces by a factor of two the dynamic range of POS. However, it would be easy to modify the recording to measure the full (LP +) (LP −) differential voltage.

6. Conclusions

We have shown that STS-1 seismometers provide a voltage POS which can be used for tidal studies because of a good signal/noise ratio. If it is possible to take care of the following conditions, the network of STS-1 seismometers, which were designed originally for seismology, could be used in gravimetry (although superconducting gravimeters or LaCoste–Romberg tidemeters with

electrostatic feedback are still superior in the tidal frequency bands: (1) improved calibration; (2) better thermal shielding and temperature stability; (3) recording of the differential signal instead of POS; (4) better adjustment of the amplitude signal to the digitization range; (5) use of an analog-to-digital converter with more than 12 bits; (6) anti-aliasing filtering to remove seismic short periods; (7) cancellation of the clock drift with a real-time reset or the use of a very accurate clock; (8) reduction of the number of gaps; (9) systematic recording of the seismometer temperature and the atmospheric pressure. This would be of great interest for global geodynamic studies, because of the huge amount of data potentially available, from locations throughout the world.

Acknowledgements

We thank the referees for their useful comments and suggestions, especially W. Zürn for his thorough review, which helped to improve this paper significantly.

References

Agnew, D.C. and Berger, J., 1978. Vertical seismic noise at very low frequencies. J. Geophys. Res., 83 (B11): 5420–5424.

Bernard, P., Karczewski, J.F., Morand, M., Dole, B. and Romanowicz, B., 1991. The G-calibration: a new method for an absolute in situ calibration of long-period accelerometers, tested on the Streckeisen instruments of the GEOSCOPE network. Bull. Seismol. Soc. Am., 81 (4): 1360–1372.

Cummins, P., Wahr, J.M., Agnew, D.C. and Tamura, Y., 1991. Constraining core undertones using stacked IDA gravity records. Geophys. J. Int., 106: 189–198.

Dehant, V. and Ducarme, B., 1987. Comparison between the theoretical and observed tidal gravimetric factors. Phys. Earth Planet. Inter., 49: 192–212.

Ducarme, B., van Ruymbeke, M. and Poitevin, C., 1986. Three years of registration with a superconducting gravimeter at the Royal Observatory of Belgium. In: R. Vieira (Editor), Proc. 10th Int. Symp. Earth Tides, Cons. Sup. Inv. Cient., Madrid, pp. 113–130.

Florsch, N., Hinderer, J., Crossley, D.J., Legros, H. and Valette, B., 1991. Preliminary spectral analysis of the residual signal of the superconducting gravimeter below one day period. Phys. Earth Planet. Inter., 68: 85–96.

Hinderer, J., 1990. Recueil de 1024 poèmes 'Gravitons et Litrons'. Editions du 'Peigne Acoustique', Obersouffelweyersheim, Alsace, France.

Hinderer, J. and Legros, H., 1989. Elasto-gravitational deformation relative gravity changes and Earth dynamics. Geophys. J., 97: 481–495.

Hinderer, J., Florsch, N., Mäkinen, J., Legros, H. and Faller, J., 1991. On the calibration of a superconducting gravimeter using absolute gravity measurements. Geophys. J. Int., 106: 491–497.

Melchior, P., 1978. The Tides of the Planet Earth. Pergamon, Oxford, 609 pp.

Melchior, P. and de Becker, M., 1983. Discussion of worldwide measurements of tidal gravity with respect to oceanic interactions, lithospheric heterogeneities, Earth's flattening and inertial forces. Phys. Earth Planet. Inter., 31: 27–53.

Pillet, R., Cantin, J.-M. and Rouland, D., 1990. Dispositif d'enregistrement pour sismomètre large bande. Géodynamique, 5: 111–119.

Richter, B., 1986. The spectrum of the registration with a superconducting gravimeter. In: R. Vieira (Editor), Proc. 10th Int. Symp. Earth Tides. Cons. Sup. Inn. Cient., Madrid, pp. 131–140.

Romanowicz, B., Cara, M., Fels, J.-F. and Rouland, D., 1984. GEOSCOPE: a French initiative in long-period three-component global seismic networks. Eos, 65 (42): 753–754.

Romanowicz, B., Karczewski, J.-F., Cara, M., Bernard, P., Borsenberger, J., Cantin, J.-M., Dole, B., Fouassier, D., Koenig, J.-C., Morand, M., Pillet, R., Pyrolley, A. and Rouland, D., 1991. The GEOSCOPE program: present status and perspectives. Bull. Seismol. Soc. Am., 81 (1): 243–264.

Rydelek, P., Zürn, W. and Hinderer, J., 1991. On tidal gravity, heat flow and lateral heterogeneities. Phys. Earth Planet. Inter., 68: 215–229.

Schüller, K., 1985. Simultaneuous tidal and multi-channel input analysis as implemented in the HYCON method. In: R. Vieira (Editor), Proc. 10th Int. Symp. Earth Tides, Cons. Sup. Inv. Cient., Madrid, pp. 515–520.

Tull, J.E., et al., 1987. SAC—seismic analysis code. Lawrence Livermore National Laboratory, Livermore, CA.

Wahr, J.M., 1981. Body tides of an elliptical, rotating, elastic and oceanless earth. Geophys. J. R. Astron. Soc., 64: 677–703.

Wenzel, H.G., Zürn, W. and Baker, T.F., 1991. In situ calibration of LaCoste–Romberg gravimeter ET19 at BFO Schiltach. Bull. Inf. Mar. Terrestr., 109: 7849–7863.

Wielandt, E. and Steim, J.M., 1985. A digital very-broad-band seismograph. Ann. Geophys., 4(B): 227–232.

Wielandt, E. and Streckeisen, G., 1982. The leaf-spring seismometer: design and performance. Bull. Seismol. Soc. Am., 72(6): 2349–2367.

Zürn, W., Wenzel, H.-G. and Laske, G., 1991. High quality data from LaCoste–Romberg gravimeter with electrostatic feedback: a challenge for superconducting gravimeters. Bull. Inf. Mar. Terrestr., 110: 7940–7952.